1-1-2017

The P2X7 receptor is not essential for development of imiquimod-induced psoriasis-like inflammation in mice

Nicholas Geraghty
University of Wollongong, ng646@uowmail.edu.au

Kylie J. Mansfield
University of Wollongong, kylie@uow.edu.au

Stephen J. Fuller
University of Sydney

Debbie Watson
University of Wollongong, dwatson@uow.edu.au

Ronald Sluyter
University of Wollongong, rsluyter@uow.edu.au

The P2X7 receptor is not essential for development of imiquimod-induced psoriasis-like inflammation in mice

Abstract

Psoriasis is a chronic inflammatory skin disorder, characterised by epidermal hyperplasia (acanthosis) and leukocyte infiltration of the skin. Current therapies are inadequate, highlighting the need for new therapeutic targets. The P2X7 receptor is implicated in the pathogenesis of psoriasis. This study investigated the role of P2X7 in imiquimod (IMQ)-induced psoriasis-like inflammation. Topically applied IMQ caused twofold greater ear swelling in BALB/c mice compared to C57BL/6 mice, which encode a partial loss-of-function missense mutation in the P2RX7 gene. However, there was no difference in histological skin pathology (acanthosis and leukocyte infiltration) between the two strains. IMQ treatment up-regulated P2X7 expression in skin from both mouse strains. Additionally, IMQ induced ATP release from cultured human keratinocytes, a process independent of cell death. Injection of the P2X7 antagonist Brilliant Blue G (BBG) but not A-804598 partly reduced ear swelling compared to vehicle-injected control mice. Neither antagonist altered skin pathology. Moreover, no difference in ear swelling or skin pathology was observed between C57BL/6 and P2X7 knock-out (KO) mice. Flow cytometric analysis of IMQ-treated skin from C57BL/6 and P2X7 KO mice demonstrated similar leukocyte infiltration, including neutrophils, macrophages and T cells. In conclusion, this study demonstrates that P2X7 is not essential for development of IMQ-induced psoriasis-like inflammation but does not exclude a role for this receptor in psoriasis development in humans or other mouse models of this disease.

Disciplines

Medicine and Health Sciences

Publication Details

Geraghty, N. J., Mansfield, K. J., Fuller, S. J., Watson, D. & Sluyter, R. (2017). The P2X7 receptor is not essential for development of imiquimod-induced psoriasis-like inflammation in mice. Purinergic Signalling, 13 (4), 405-415.

The P2X7 receptor is not essential for development of imiquimod-induced psoriasis-like inflammation in mice

Nicholas J Geraghty [1 2 3], Kylie J Mansfield [3 4], Stephen J Fuller [5], Debbie Watson[* 1 2 3] and Ronald Sluyter[* 1 2 3]

[1] School of Biological Sciences, University of Wollongong, Wollongong, NSW, Australia, [2] Centre for Medical and Molecular Biosciences, University of Wollongong, Wollongong, NSW, Australia, [3] Illawarra Health and Medical Research Institute, Wollongong, NSW, Australia, [4] Graduate School of Medicine, University of Wollongong, Wollongong, NSW, Australia, [5] Sydney Medical School, University of Sydney, Sydney, NSW

Correspondence to: Ronald Sluyter, Associate Professor, School of Biological Sciences, University of Wollongong, Illawarra Health and Medical Research Institute, Wollongong, NSW 2522, Australia. Email address: rsluyter@uow.edu.au

* Debbie Watson and Ronald Sluyter are co-senior authors

ABSTRACT

Psoriasis is a chronic inflammatory skin disorder, characterised by epidermal hyperplasia (acanthosis) and leukocyte infiltration of the skin. Current therapies are inadequate, highlighting the need for new therapeutic targets. The P2X7 receptor is implicated in the pathogenesis of psoriasis. This study investigated the role of P2X7 in imiquimod (IMQ)-induced psoriasis-like inflammation. Topically-applied IMQ caused two-fold greater ear swelling in BALB/c mice compared to C57BL/6 mice, which encode a partial loss-of-function missense mutation in the *P2RX7* gene. However, there was no difference in histological skin pathology (acanthosis and leukocyte infiltration) between the two strains. IMQ treatment up-regulated P2X7 expression in skin from both mouse strains. Additionally, IMQ induced ATP release from cultured human keratinocytes, a process independent of cell death. Injection of the P2X7 antagonist Brilliant Blue G (BBG) but not A-804598 partly reduced ear swelling compared to vehicle-injected control mice. Neither antagonist altered skin pathology. Moreover, no difference in ear swelling or skin pathology was observed between C57BL/6 and P2X7 knock-out (KO) mice. Flow cytometric analysis of IMQ-treated skin from C57BL/6 and P2X7 KO mice demonstrated similar leukocyte infiltration, including neutrophils, macrophages and T cells. In conclusion, this study demonstrates that P2X7 is not essential for development of IMQ-induced psoriasis-like inflammation, but does not exclude a role for this receptor in psoriasis development in humans or other mouse models of this disease.

KEYWORDS: P2X7 receptor, extracellular ATP, imiquimod, psoriasis, skin immune system

INTRODUCTION

Psoriasis affects 1-3% of the general population of Western countries, reducing quality of life and posing a significant economic burden [1]. In the USA alone, psoriasis is estimated to cost $112 billion per year [2]. Inflammation and hyper-proliferation of keratinocytes in psoriasis results in epidermal hyperplasia (acanthosis) and plaque- or pustular-like skin lesions [3]. This characteristic inflammation is driven by infiltrating leukocytes, including neutrophils, macrophages and T cells [4]. These leukocytes exert their effects by release of pro-inflammatory cytokines such as interferon gamma (IFN-γ) [3,4], which promotes the hyper-proliferation of keratinocytes, with the resulting cell damage exacerbating inflammation and leading to plaque formation [4].

The imiquimod (IMQ)-induced psoriasis-like inflammation mouse model is a valuable model for studying psoriasis pathogenesis. This model involves application of Aldara^{TM} cream, containing IMQ, which causes epidermal hyperplasia and immune infiltration similar to psoriasis in humans [5]. IMQ treatment results in scaling and thickening of skin as well as infiltration of immune cells 48-72 hours after first application [5]. This model has been well characterised [6] and used in some 200 different studies to date [7].

The ATP-gated P2X7 receptor channel has been implicated in a number of skin diseases including psoriasis [8]. P2X7 is present on keratinocytes [9] and immune cells important in psoriasis including neutrophils [10], macrophages [11] and T cells [12], where its activation can drive cytokine release and potentially promote inflammation [8]. Notably, IFN-γ can up-regulate the expression of P2X7 in primary keratinocytes [13] and P2X7 expression is increased in human psoriatic lesions [13,14]. A functional role for P2X7 in psoriasis has also been suggested. Injection of the P2X7 agonist 3'-O-(4-benzoyl)benzoyl ATP into normal human skin explants induces increased expression of cytokines and other molecules commonly associated with psoriasis, including interleukin (IL)-1β, IL-6 and tumour necrosis

factor alpha (TNF-α) [14]. Importantly, these responses could be prevented through pharmacological blockade of P2X7 [14]. P2X7 activation of skin migrating dendritic cells also promoted Th17 responses [14], a T cell subtype known to contribute to psoriasis pathogenesis [15].

This study investigated the role of P2X7 in the pathogenesis of psoriasis using a murine model of IMQ-induced psoriasis-like inflammation. Results indicate that P2X7 is up-regulated in psoriatic skin in both BALB/c and C57BL/6 mice, which encode the wild-type (P451) or partial loss-of function (451L) allele, respectively [16]. IMQ also induced ATP release from human keratinocytes. However, pharmacological blockade or genetic deletion of P2X7 showed a limited role for P2X7 in this murine model of psoriasis.

MATERIALS AND METHODS

Cells

Human HaCaT keratinocytes and murine J774 macrophages were obtained and cultured as described [17,18]. Cell lines were checked for *Mycoplasma spp.* infections every two months, using a MycoAlert™ Mycoplasma detection kit (Lonza, Basal, Switzerland) as per the manufacturer's instructions. Cells were routinely negative for *Mycoplasma spp.*

Mice

Female and male mice (aged 6-10 weeks) were used in experiments conducted under protocol AE14/10, which was approved by the University of Wollongong Animal Ethics Committee (Wollongong, Australia). BALB/c and C57BL/6 mice were obtained from Australian BioResources (Moss Vale, Australia). P2X7 knock-out (KO) mice [19] backcrossed onto a C57BL/6 background [20], were maintained at the University of Wollongong and genotyped as described [19]. All mice were housed in open top cages and provided with food and water, *ad libitum*. All mice were housed in a temperature-controlled environment with a 12 h light/12 h dark cycle.

Murine model of IMQ-induced psoriasis-like inflammation

A total of 25 mg of Aldara™ cream (1.25 mg IMQ) (iNova Pharmaceuticals, Thornleigh, Australia) was applied to both sides of one ear of each mouse and the contralateral ear remained untreated (control) (days 0-5) as described [21]. Prior to treatment mice were weighed and ear measurements were recorded using Interapid (Rolle, Switzerland) spring-loaded calipers (days 0-6). In some experiments, Brilliant Blue G (BBG) or A-804598 (both Sigma-Aldrich, St Louis, MO, USA) (final concentration 50 mg/kg in mice), and their

respective diluent controls (saline or dimethyl sulfoxide (DMSO), respectively), were injected every second day (as indicated). Mice were sacrificed on day 6 and ears collected.

Histological analysis

Ears from euthanised mice were incubated overnight in neutral buffered (10%) formalin (Sigma-Aldrich). Fixed tissues were removed, embedded in paraffin, sectioned (5 μm) and stained with haematoxylin and eosin (POCD, Artarmon, Australia). Histology was observed using a Leica (Wetzlar, Germany) DM500 inverted light microscope, with images captured and processed using Leica application suite software version 4.7. Acanthosis (epidermal thickness) was measured using ImageJ software version 1.48 (National Institutes of Health, Bethesda, MD, USA).

Isolation of RNA and cDNA synthesis

Ears from euthanised mice were stored in RNAlater (Sigma-Aldrich) at -20°C until required. RNA was isolated using the ISOLATE II RNA Mini Kit (Bioline, London, UK) as per the manufacturer's instructions. Briefly, tissue in lysis buffer containing 1% (v/v) β-mercaptoethanol (Sigma-Aldrich) was homogenised (two 20 second cycles at 5500 rpm) in a Bertin Technologies (Montigny-le-Bretonneux, France) Precellys 24 tissue homogeniser. Isolated RNA was immediately converted to cDNA using the qScript cDNA Synthesis Kit (Quanta Biosciences, Gaithersburg, MD, USA) as per the manufacturer's instructions. cDNA was checked by PCR amplification of the house keeping gene glyceraldehyde 3-phosphate dehydrogenase (Invitrogen, Carlsbad, CA, USA) for 35 cycles at 95°C for 1 min, 55°C for 1 min and 72°C for 1 min and a holding temperature of 4°C. Purity and size of amplicons were confirmed by a 2% agarose gel electrophoresis.

Quantitative real-time polymerase chain reaction

qPCR reactions were performed using TaqMan Universal Master Mix II (Thermo Fisher Scientific, Waltham, Massachusetts, USA) according to the manufacturer's instructions with primers for FAM-labelled GAPDH (Mm99999915_g1) and VIC-labelled *P2RX7* (Mm01199503_m1) (Thermo Fisher Scientific). qPCR cycles consisted of an initial step of 50°C for 2 min, followed by 50°C for 10 min, and 40 cycles at 95°C for 15 s, and 60°C for 1 min. qPCR reactions were conducted in triplicate on a Roche Diagnostics (Indianapolis, IN, USA) LightCycler 480 and analysis was conducted using LightCycler480 software version 1.5.1.

ATP release assay

ATP release assays were performed as described [22]. Briefly, HaCaT keratinocytes were plated in 12-well plates (Greiner Bio-One, Frickenhausen, Germany) at a concentration of 2 x 10^5 cells/well in RPMI 1640 medium containing 2 mM L-glutamine, 1% non-essential amino acids (all Thermo Fisher Scientific), and 10% (v/v) heat-inactivated foetal bovine serum (Bovogen Biologicals, Keller East, Australia), and incubated for 24 h at 37°C/5% CO_2. Cells were washed thrice with PBS (Thermo Fisher Scientific), and incubated in 1 mL PBS containing DMSO or 1 μg/mL IMQ (Sigma-Aldrich) in DMSO for 30 min at 37°C/5% CO_2. The final concentration of DMSO in both groups was 0.1%. Cells were then centrifuged through 10% bovine serum albumin (4,000 x g for 3 min) and cell free supernatants were stored in duplicate at -20°C until required. ATP concentrations in supernatants were assessed using a Bioluminescence ATP Assay Kit (Sigma-Aldrich) as described [23]. The amount of lactate dehydrogenase (LDH) in supernatants was determined using a Cytotoxicity Detection Kit (LDH) (Roche Diagnostics) as per the manufacturer's instructions using a Molecular devices (Sunnyvale, CA, USA) Spectramax Plus 384 plate reader.

ATP-induced ethidium$^+$ uptake assay

P2X7 pore formation was quantified by measuring ATP-induced ethidium$^+$ uptake as described [24]. Briefly, J774 cells in NaCl medium (145 mM NaCl, 5 mM KCl, 5 mM glucose and 10 mM HEPES, pH 7.5) were pre-incubated in the absence or presence of BBG or A-804598 (as indicated) for 15 min at 37°C. Cells were then incubated with 25 µM ethidium bromide (Sigma-Aldrich) in the absence or presence of 1 mM ATP (Sigma-Aldrich) for 10 min. Incubations were stopped by addition of ice-cold NaCl medium containing 20 mM $MgCl_2$ ($MgCl_2$ medium) and cells were washed with NaCl medium (300 x g for 3 min). Data was collected using a BD Biosciences (San Jose, CA, USA) LSRFortessa X-20 flow cytometer (using band-pass filter 530/30 for ethidium$^+$) and FACSDiva software version 8.0. Mean fluorescence intensity (MFI) of ethidium$^+$ uptake was analysed using FlowJo software version 8.7.1. (TreeStar Inc., Ashland, OH, USA).

Immunophenotyping

CD16/32 Fc Block (clone 2-4G2), Brilliant Violet (BV)450-conjugated rat anti-mouse Ly-6G (clone 1A8), peridinin chlorophyll protein (PerCP)-conjugated rat anti-mouse CD4 (clone RM4.5), allophycocyanin (APC)-conjugated rat anti-mouse CD45 (clone 30-F11) and R-phycoerythrin (PE)-Cy7 conjugated hamster anti-mouse CD3e (clone 145-2C11) were from BD Biosciences. PE-conjugated rat anti-mouse CD11b (clone M1/70) was from BioLegend (San Diego, CA, USA).

Enzymatic digestion of ears was performed as described [25]. Briefly, dorsal and ventral sides of ears were separated and incubated in 20 mM EDTA (Sigma-Aldrich) in Tris-buffered saline (pH 7.3) for 2 hours at 37°C. Epidermal and dermal layers were mechanically separated, cut into smaller fragments using a scalpel and homogenised in RPMI 1640 medium containing 1 mg/mL collagenase IV and 15 U/mL DNase I (both Sigma-Aldrich),

and 5% heat-inactivated foetal bovine serum at room temperature for 90 min with agitation. Enzymatic digestion was stopped by addition of 100 mM EDTA and suspensions filtered through 70 μm cell strainers (Falcon, Franklin, NJ, USA). Cells were centrifuged (300 x g for 5 min), resuspended in PBS and counted manually using a Boeco (Hamburg, Germany) Neubauer Improved Bright Line haemacytometer. Cells were incubated with CD16/32 Fc Block for 10 min and then with fluorochrome-conjugated monoclonal antibodies in the dark for 10 min. Cells were washed twice with PBS (300 x g for 3 min), resuspended in PBS and data was collected using a LSRFortessa X-20 flow cytometer (using band pass filters 450/50 for BV421, 695/40-A for PerCP, 575/25-A for PE, 780/60 for PE-Cy7 and 670/30 for APC) and FACSDiva software. The relative percentage of cells was analysed using FlowJo software.

Statistical Analysis

Data is given as mean ± standard error of the mean (SEM). Statistical differences were calculated using Student's t test for single comparisons or one-way analysis of variance (ANOVA) with Tukeys post-hoc test for multiple comparisons. Weight and ear measurements were analysed using a repeated measures two-way ANOVA. All statistical analyses and graphs were generated using Prism 5 for Windows software (GraphPad Software, La Jolla, CA, USA).

RESULTS

IMQ treatment induces greater ear swelling in BALB/c mice compared to C57BL/6 mice

To investigate the role of P2X7 in psoriasis, IMQ-induced psoriasis-like inflammation was first compared over 6 days in BALB/c and C57BL/6 mice. C57BL/6 mice encode a loss-of-function mutation (P451L) in the *P2RX7* gene, while BALB/c mice are wild-type at this allele [16]. IMQ induced ear swelling in ears relative to control (contralateral untreated) ears from day 3 in both strains (Fig. 1a). However, IMQ-induced ear swelling was greater in BALB/c mice compared to C57BL/6 mice over 6 days ($P < 0.0001$) (Fig. 1a). Histological analysis of IMQ-treated ears from BALB/c and C57BL/6 mice demonstrated acanthosis (epidermal thickening) and leukocyte infiltration compared to control ears; however, there was no difference between strains (Fig. 1b). Image analysis of histological sections revealed that epidermal thickness was significantly greater in IMQ-treated ears compared to control ears from both BALB/c mice ($P < 0.0001$) and C57BL/6 mice ($P < 0.0001$). However, IMQ-induced epidermal thickening did not significantly differ between the two strains (Fig. 1c).

P2X7 mRNA is up-regulated in IMQ-induced psoriatic lesions and IMQ induces ATP release from keratinocytes

Next, P2X7 mRNA expression in IMQ-treated and control ears was analysed by qPCR. P2X7 was significantly up-regulated almost three-fold and two-fold in IMQ-treated ears compared to control ears from BALB/c mice ($P = 0.0002$) and C57BL/6 mice ($P = 0.0343$), respectively (Fig. 2a). To further determine a potential role for P2X7 activation in IMQ-induced psoriasis-like inflammation, HaCaT keratinocytes were incubated in the presence of

1 μg/mL IMQ or DMSO (vehicle control) for 30 min and the amount of ATP released measured using a bioluminescence assay. IMQ induced significantly greater amounts of ATP release compared to DMSO (P = 0.0425) (Fig. 2b). To examine if this ATP release was due to cytotoxicity by IMQ, the relative amount of LDH in the above supernatants was determined using a spectrophotometric assay. Although the absorbance in the IMQ cells was reduced the absorbance values were not significantly different between IMQ and control groups (Fig. 2c).

BBG does not prevent IMQ-induced psoriasis-like inflammation

To investigate the role of P2X7 in IMQ-induced psoriasis-like inflammation, the P2X7 antagonist BBG [26] was used in this model. First, to confirm that BBG can impair murine P2X7 activation, J774 macrophages, which express functional P2X7 [27], were pre-incubated in the absence or presence of 10 μM BBG and ATP-induced cation dye uptake was measured by flow cytometry. BBG significantly reduced ATP-induced ethidium$^+$ uptake by 87% (P < 0.0001) (Fig. 3a). To determine if BBG could prevent the development of IMQ-induced psoriasis-like inflammation BALB/c mice were treated with IMQ as above and injected with BBG or saline (vehicle control) every second day (days 0, 2 and 4). IMQ induced ear swelling in mice from day 3 regardless of treatment. However, IMQ-induced ear swelling was partially reduced (by 21%) in BBG-injected mice compared to saline-injected mice over 6 days (P = 0.0068) (Fig. 3b). Histological analysis of IMQ-treated ears from BBG- and saline-injected mice demonstrated epidermal thickening and leukocyte infiltration compared to control ears; but there were no differences between BBG and saline treatments (Fig. 3c). Image analysis of histological sections revealed that epidermal thickness was greater in IMQ-treated ears compared to control ears from BBG-injected mice (P < 0.0001) and saline-

injected mice ($P < 0.0001$). Epidermal thickness in IMQ-treated and control ears was similar between BBG and saline treatments (Fig. 3d).

A-804598 does not prevent IMQ-induced psoriasis-like inflammation

To further examine the potential effects of P2X7 blockade on psoriasis-like inflammation, the P2X7 antagonist A-804598 [28] was used. Similar to BBG, A-804598 near-completely abrogated ATP-induced ethidium$^+$ uptake in J774 macrophages ($P < 0.0001$) (Fig. 4a). BALB/c mice were treated with IMQ as above and injected with A-804598 or DMSO (vehicle control) every second day (days 0 and 2). IMQ induced ear swelling in mice from day 3 regardless of treatment. A-804598- and DMSO-injected mice demonstrated similar ear swelling (Fig. 4b). Histological analysis of IMQ-treated ears from A-804598-injected and DMSO-injected mice demonstrated epidermal thickening and leukocyte infiltration compared to control ears with no difference between A-804598 and control treatments (Fig. 4c). Image analysis of histological sections revealed that epidermal thickness was greater in IMQ-treated ears compared to control ears from A-804598-injected mice ($P < 0.0001$) and DMSO-injected mice ($P < 0.0001$). Epidermal thickness in IMQ-treated and control ears was also similar between A-804598 and control treatments (Fig. 4d).

Genetic deletion of P2X7 does not prevent IMQ-induced psoriasis-like inflammation

Finally, to determine if genetic deficiency of P2X7 could alter IMQ-induced psoriasis-like inflammation, C57BL/6 and P2X7 KO mice were treated with IMQ as above. Both C57BL/6 and P2X7 KO mice demonstrated ear swelling in IMQ-treated ears from day 3, but this was not significantly different between the two strains over 6 days (Fig. 5a). Histological analysis of IMQ-treated ears from C57BL/6 and P2X7 KO mice demonstrated epidermal thickening and leukocyte infiltration compared to control ears, with no difference between strains (Fig.

5b). Image analysis of histology revealed that epidermal thickness was significantly greater in IMQ-treated ears compared to control ears from C57BL/6 mice ($P < 0.0001$) and P2X7 KO mice ($P < 0.0001$). Epidermal thickness in IMQ-treated and control ears was also similar between C57BL/6 and P2X7 KO mice (Fig. 5c).

IMQ-induced leukocyte infiltration is similar in C57BL/6 and P2X7 KO mice

The data above indicates that P2X7 deficiency does not prevent IMQ-induced psoriasis-like inflammation in mice. However, the possibility remained that P2X7 deficiency may have altered the number of leukocyte subsets infiltrating the skin in this disease model. Therefore, whole ear cell suspensions of IMQ-treated and control ears from C57BL/6 and P2X7 KO mice were examined by flow cytometry. IMQ induced a significant increase in total skin leukocytes in both C57BL/6 ($P = 0.0002$) and P2X7 KO ($P = 0.0029$) mice, but there was no significant difference between strains (Figure 6a). Subset analysis also revealed IMQ induced a significant increase in neutrophils and macrophages in both C57BL/6 ($P = 0.0027$ and $P < 0.0001$, respectively) and P2X7 KO ($P = 0.0020$ and $P = 0.0046$, respectively) mice, but there was no significant difference between strains (Figure 6b-c). IMQ induced a significant increase in T cells in C57BL/6 ($P = 0.0006$) but not P2X7 KO mice; yet there was no significant difference between strains (Figure 6d).

DISCUSSION

This study demonstrated that P2X7 is not essential for the development of IMQ-induced psoriasis-like inflammation in mice. With the exception of a partial effect on ear swelling by BBG, pharmacological blockade or genetic deletion of P2X7 did not impact development of IMQ-induced psoriasis-like inflammation. The general lack of effect of either P2X7 antagonist was not due to the preparations of BBG or A-804598, as both compounds blocked ATP-induced dye uptake into murine macrophages in this study. Moreover, both compounds were used *in vivo* at concentrations known to inhibit murine P2X7 [29]. In regards to IMQ-induced ear swelling, BBG may be blocking alternate molecules, such as P2X1 [30], P2X5 [31], the ATP channel pannexin-1 [32] or a voltage-gated sodium channel [33].

Genetic deficiency of P2X7 did not impact leukocyte infiltration in IMQ-induced psoriasis-like inflammation. In contrast, a previous study reported that P2X7 KO mice had reduced neutrophil infiltration into skin in a croton oil model of irritant contact dermatitis [34]. However, in line with our current study, ear swelling was similar between wild-type and P2X7 KO mice in croton oil-induced irritant contact dermatitis [34,35]. Conversely, P2X7 KO mice are protected from allergic contact dermatitis, which was also assessed by ear swelling measurements [35]. This previous study demonstrated that P2X7-mediated IL-1β release, which requires NLRP3 inflammasome activation [36], was essential for allergic contact dermatitis [35]. In contrast, activation of the NLRP3 inflammasome is not required for IMQ-induced psoriasis-like inflammation [37]. Thus, this provides a possible explanation as to why P2X7 is not essential in this model of psoriasis. Collectively, this indicates P2X7 plays differing roles in various inflammatory skin disorders, but given previous findings [13,14] further investigation of P2X7 in human psoriasis and other mouse models of this disease is warranted. Moreover, it should be noted that C-terminal truncated P2X7 variants are present at low amounts in C57BL/6 and Pfizer P2X7 KO mice [38], the same strains used

in the current study. Although P2X7-induced pore formation is absent in splenic T and B cells [39], epidermal Langerhans cells and keratinocytes [20] from these P2X7 KO mice, a role for these escape P2X7 variants in IMQ-induced psoriasis-like inflammation in P2X7 KO mice cannot be excluded. P2X7 KO strains in which escape variants have not been reported, such as those from Lexicon Pharmaceuticals [40] or conditional humanised P2X7 KO mice [41], provide alternatives to assess the potential role of P2X7 in psoriasis.

Ear swelling, but not histological acanthosis or inflammation, differed between BALB/c and C57BL/6 mice. Thus, this difference in ear swelling most likely reflects differences in oedema. Coincidentally, this difference in ear swelling corresponds to *P2RX7* genotype (P451L mutation), but P2X7 deficiency in mice on a C57BL/6 background does not alter ear swelling compared to wild-type C57BL/6 mice. This suggests that the difference between BALB/c and C57BL/6 mice is not due to reduced P2X7 activity as a result of the P451L mutation in C57BL/6 mice. In this regard, whilst some have reported that the P451L mutation results in a loss of P2X7 activity [16,42], others have observed no differences in the activity or pharmacological profiles between recombinant BALB/c and C57BL/6 P2X7 [43]. Moreover, it remains to be established if P2X7 variants differ between BALB/c and C57BL/6 mice, and if P2X7 activity differs between these two mouse strains *in vivo*. BALB/c and C57BL/6 mice have a diverse lineage and display phenotypic and genetic differences [44,45]. Thus, differences in IMQ-induced ear swelling between these strains could be due to any number of genotypic or phenotypic differences. Notably, IL-22 expression is increased in IMQ-induced psoriasis-like inflammation in BALB/c, but not C57BL/6, mice [5]. Conversely, IL-6 is detected in C57BL/6 mice, but not BALB/c mice [5]. Thus, a role for these cytokines in oedema during psoriasis warrants further investigation.

Analysis by qPCR revealed P2X7 mRNA expression was up-regulated in IMQ-treated skin in both BALB/c and C57BL/6 mice. Although, it was not determined if P2X7 protein is

increased in these mice, P2X7 protein is increased in lesional skin from psoriasis patients [13,14]. Notably, P2X7 is up-regulated on human keratinocytes by IFN-γ [13], a cytokine implicated in psoriasis pathogenesis [46] including IMQ-induced psoriasis-like inflammation [5]. Therefore, P2X7 may be up-regulated on keratinocytes due to IFN-γ present in IMQ-treated skin. Alternatively, since P2X7 is also found on various skin immune cells [8], increased P2X7 expression in IMQ-treated ears may simply reflect increased numbers of infiltrating leukocytes in IMQ-induced skin as observed in the current study.

Finally, this study demonstrated that HaCaT keratinocytes can constitutively release ATP, as previously observed [47], and that this release could be increased by IMQ. The IMQ-induced ATP release was not due to cytotoxicity, as IMQ did not significantly alter LDH release. Although genetic deletion or pharmacological blockade of P2X7 did not impact IMQ-induced psoriasis-like inflammation in this study, extracellular ATP may be involved in the development of this disease through activation of purinergic receptors other than P2X7. In particular, P2Y1, P2Y2 and P2Y6 have been implicated in psoriasis or other inflammatory skin conditions [48].

In conclusion, pharmacological blockade and genetic deletion of P2X7 could not prevent IMQ-induced psoriasis-like inflammation. However, given the potential roles of P2X7 in human psoriasis [13,14] and other skin diseases [8], a role for this receptor in human psoriasis or other mouse models of this disease cannot be excluded.

ACKNOWLEDGEMENTS

The authors thank Vanessa Sluyter (University of Wollongong, Wollongong, Australia) and Illawarra Health and Medical Research Institute technical and animal staff for technical support. The authors also thank Chao Deng, Blagojce Jovcevski (both University of Wollongong, Wollongong, Australia) and Scott Byrne (University of Sydney, Sydney,

Australia) for helpful advice and iNova Pharmaceuticals for kindly donating some Aldara™ cream samples.

This project was funded by the Faculty of Science, Medicine and Health, University of Wollongong. NJ Geraghty is supported through an Australian Government Research Training Program Scholarship. D Watson is supported by AMP's Tomorrow Fund. D Watson and R Sluyter receive additional support from the Centre for Medical and Molecular Bioscience, University of Wollongong.

CONFLICT OF INTEREST:

The authors wish to declare that there are no conflicts of interest.

REFERENCE LIST

1 Lebwohl, M. G., Bachelez, H., Barker, J. *et al.* (2014) Patient perspectives in the management of psoriasis: Results from the population-based Multinational Assessment of Psoriasis and Psoriatic Arthritis Survey. JAMA Dermatol 70 (5):871-881.e830. 10.1016/j.jaad.2013.12.018

2 Brezinski, E. A., Dhillon, J. S. & Armstrong, A. W. (2015) Economic burden of psoriasis in the United States a systematic review. JAMA Dermatol 151 (6):651-658. 10.1001/jamadermatol.2014.3593

3 Nestle, F. O., Kaplan, D. H. & Barker, J. (2009) Mechanisms of disease: Psoriasis. N Engl J Med 361 (5):496-509. 10.1056/NEJMra0804595

4 Nestle, F. O., Di Meglio, P., Qin, J. Z. & Nickoloff, B. J. (2009) Skin immune sentinels in health and disease. Nat Rev Immunol 9 (10):679-691. 10.1038/nri2622

5 Van Der Fits, L., Mourits, S., Voerman, J. S. A. *et al.* (2009) Imiquimod-induced psoriasis-like skin inflammation in mice is mediated via the IL-23/IL-17 axis. J Immunol 182 (9):5836-5845. 10.4049/jimmunol.0802999

6 Flutter, B. & Nestle, F. O. (2013) TLRs to cytokines: Mechanistic insights from the imiquimod mouse model of psoriasis. Eur J Immunol 43 (12):3138-3146. 10.1002/eji.201343801

7 Hawkes, J. E., Gudjonsson, J. E. & Ward, N. L. (2017) The Snowballing Literature on Imiquimod-Induced Skin Inflammation in Mice: A Critical Appraisal. J Invest Dermatol 137 (3):546-549. 10.1016/j.jid.2016.10.024

8 Geraghty, N. J., Watson, D., Adhikary, S. R. & Sluyter, R. (2016) P2X7 receptor in skin biology and diseases. World J Dermatol 5 (2):72-83. 10.5314/wjd.v5.i2.72

9 Greig, A. V. H., Linge, C., Cambrey, A. & Burnstock, G. (2003) Purinergic Receptors Are Part of a Signaling System for Keratinocyte Proliferation, Differentiation, and Apoptosis in Human Fetal Epidermis. J Invest Dermatol 121 (5):1145-1149. 10.1046/j.1523-1747.2003.12567.x

10 Karmakar, M., Katsnelson, M. A., Dubyak, G. R. & Pearlman, E. (2016) Neutrophil P2X7 receptors mediate NLRP3 inflammasome-dependent IL-1β secretion in response to ATP. Nat Commun 7 10555. 10.1038/ncomms10555

11 De Torre-Minguela, C., Barberà-Cremades, M., Gómez, A. I., Martín-Sánchez, F. & Pelegrín, P. (2016) Macrophage activation and polarization modify P2X7 receptor secretome influencing the inflammatory process. Sci Rep 6 22586. 10.1038/srep22586

12 MacLeod, A. S., Rudolph, R., Corriden, R., Ye, I., Garijo, O. & Havran, W. L. (2014) Skin-resident T cells sense ultraviolet radiation-induced injury and contribute to DNA repair. J Immunol 192 (12):5695-5702. 10.4049/jimmunol.1303297

13 Pastore, S., Mascia, F., Gulinelli, S. *et al.* (2007) Stimulation of purinergic receptors modulates chemokine expression in human keratinocytes. J Invest Dermatol 127 (3):660-667. 10.1038/sj.jid.5700591

14 Killeen, M. E., Ferris, L., Kupetsky, E. A., Falo Jr, L. & Mathers, A. R. (2013) Signaling through purinergic receptors for ATP induces human cutaneous innate and adaptive Th17 responses: Implications in the pathogenesis of psoriasis. J Immunol 190 (8):4324-4336. 10.4049/jimmunol.1202045

15 Zheng, Y., Danilenko, D. M., Valdez, P., Kasman, I., Eastham-Anderson, J., Wu, J. & Ouyang, W. (2007) Interleukin-22, a TH17 cytokine, mediates IL-23-induced dermal inflammation and acanthosis. Nature 445 (7128):648-651. 10.1038/nature05505

16 Adriouch, S., Dox, C., Welge, V., Seman, M., Koch-Nolte, F. & Haag, F. (2002) Cutting edge: A natural P451L mutation in the cytoplasmic domain impairs the function of the mouse P2X7 receptor. J Immunol 169 (8):4108-4112.
17 Farrell, A. W., Gadeock, S., Pupovac, A., Wang, B., Jalilian, I., Ranson, M. & Sluyter, R. (2010) P2X7 receptor activation induces cell death and CD23 shedding in human RPMI 8226 multiple myeloma cells. Biochim Biophys Acta Gen Subjects 1800 (11):1173-1182. 10.1016/j.bbagen.2010.07.001
18 Sluyter, R. & Vine, K. L. (2016) N-Alkyl-Substituted Isatins Enhance P2X7 Receptor-Induced Interleukin-1beta Release from Murine Macrophages. Mediators Inflamm 2016 2097219. 10.1155/2016/2097219
19 Solle, M., Labasi, J., Perregaux, D. G., Stam, E., Petrushova, N., Koller, B. H., Griffiths, R. J. & Gabel, C. A. (2001) Altered cytokine production in mice lacking P2X7 receptors. J Biol Chem 276 (1):125-132. 10.1074/jbc.M006781200
20 Tran, J. N., Pupovac, A., Taylor, R. M., Wiley, J. S., Byrne, S. N. & Sluyter, R. (2010) Murine epidermal Langerhans cells and keratinocytes express functional P2X7 receptors. Exp Dermatol 19 (8):e151-e157. 10.1111/j.1600-0625.2009.01029.x
21 Riol-Blanco, L., Ordovas-Montanes, J., Perro, M. *et al.* (2014) Nociceptive sensory neurons drive interleukin-23-mediated psoriasiform skin inflammation. Nature 510 (7503):157-161. 10.1038/nature13199
22 Mizumoto, N., Mummert, M. E., Shalhevet, D. & Takashima, A. (2003) Keratinocyte ATP Release Assay for Testing Skin-Irritating Potentials of Structurally Diverse Chemicals. J Invest Dermatol 121 (5):1066-1072. 10.1046/j.1523-1747.2003.12558.x
23 Mansfield, K. J. & Hughes, J. R. (2014) P2Y Receptor Modulation of ATP Release in the Urothelium. BioMed Res Int 2014 8. 10.1155/2014/830374
24 Bartlett, R., Yerbury, J. J. & Sluyter, R. (2013) P2X7 receptor activation induces reactive oxygen species formation and cell death in murine EOC13 microglia. Mediators Inflamm 2013 (18):22-40. 10.1155/2013/271813
25 Rana, S., Byrne, S. N., MacDonald, L. J., Chan, C. Y. Y. & Halliday, G. M. (2008) Ultraviolet B suppresses immunity by inhibiting effector and memory T cells. Am J Pathol 172 (4):993-1004. 10.2353/ajpath.2008.070517
26 Jiang, L.-H., Mackenzie, A. B., North, R. A. & Surprenant, A. (2000) Brilliant blue G selectively blocks ATP-gated rat P2X7 receptors. Mol Pharmacol 58 (1):82-88. 10.1124/mol.58.1.82
27 Coutinho-Silva, R., Ojcius, D. M., Górecki, D. C. *et al.* (2005) Multiple P2X and P2Y receptor subtypes in mouse J774, spleen and peritoneal macrophages. Biochem Pharmacol 69 (4):641-655. 10.1016/j.bcp.2004.11.012
28 Donnelly-Roberts, D. L., Namovic, M. T., Surber, B., Vaidyanathan, S. X., Perez-Medrano, A., Wang, Y., Carroll, W. A. & Jarvis, M. F. (2009) [3H]A-804598 ([3H]2-cyano-1-[(1S)-1-phenylethyl]-3-quinolin-5-ylguanidine) is a novel, potent, and selective antagonist radioligand for P2X7 receptors. Neuropharmacology 56 (1):223-229. 10.1016/j.neuropharm.2008.06.012
29 Bartlett, R., Stokes, L. & Sluyter, R. (2014) The P2X7 Receptor Channel: Recent Developments and the Use of P2X7 Antagonists in Models of Disease. Pharmacol Rev 66 (3):638-675. 10.1124/pr.113.008003
30 Seyffert, C., Schmalzing, G. & Markwardt, F. (2004) Dissecting individual current components of co-expressed human P2X1 and P2X7 receptors. Curr Top Med Chem 4 (16):1719-1730. 10.2174/1568026043387160

31 Bo, X., Jiang, L.-H., Wilson, H. L., Kim, M., Burnstock, G., Surprenant, A. & North, R. A. (2003) Pharmacological and Biophysical Properties of the Human $P2X_5$ Receptor. Mol Pharmacol 63 (6):1407-1416. 10.1124/mol.63.6.1407

32 Qiu, F. & Dahl, G. (2009) A permeant regulating its permeation pore: Inhibition of pannexin 1 channels by ATP. Am J Physiol Cell Physiol 296 (2):250-255. 10.1152/ajpcell.00433.2008

33 Jo, S. & Bean, B. P. (2011) Inhibition of neuronal voltage-gated sodium channels by Brilliant blue G. Mol Pharmacol 80 (2):247-257. 10.1124/mol.110.070276

34 Da Silva, G. L., Sperotto, N. D. M., Borges, T. J. *et al.* (2013) P2X7 receptor is required for neutrophil accumulation in a mouse model of irritant contact dermatitis. Exp Dermatol 22 (3):184-188. 10.1111/exd.12094

35 Weber, F. C., Esser, P. R., Müller, T. *et al.* (2010) Lack of the purinergic receptor P2X 7 results in resistance to contact hypersensitivity. J Exp Med 207 (12):2609-2619. 10.1084/jem.20092489

36 Di Virgilio, F. (2007) Liaisons dangereuses: P2X7 and the inflammasome. Trends Pharmacol Sci 28 (9):465-472. 10.1016/j.tips.2007.07.002

37 Rabeony, H., Pohin, M., Vasseur, P. *et al.* (2015) IMQ-induced skin inflammation in mice is dependent on IL-1R1 and MyD88 signaling but independent of the NLRP3 inflammasome. Eur J Immunol 45 (10):2847-2857. 10.1002/eji.201445215

38 Masin, M., Young, C., Lim, K. *et al.* (2012) Expression, assembly and function of novel C-terminal truncated variants of the mouse P2X7 receptor: Re-evaluation of P2X7 knockouts. Br J Pharmacol 165 (4):978-993. 10.1111/j.1476-5381.2011.01624.x

39 Pupovac, A., Geraghty, N. J., Watson, D. & Sluyter, R. (2015) Activation of the P2X7 receptor induces the rapid shedding of CD23 from human and murine B cells. Immunol Cell Biol 93 (1):77-85. 10.1038/icb.2014.69

40 Basso, A. M., Bratcher, N. A., Harris, R. R., Jarvis, M. F., Decker, M. W. & Rueter, L. E. (2009) Behavioral profile of P2X7 receptor knockout mice in animal models of depression and anxiety: Relevance for neuropsychiatric disorders. Behav Brain Res 198 (1):83-90. 10.1016/j.bbr.2008.10.018

41 Metzger, M. W., Walser, S. M., Aprile-Garcia, F. *et al.* (2016) Genetically dissecting P2rx7 expression within the central nervous system using conditional humanized mice. Purinergic Signalling 10.1007/s11302-016-9546

42 Young, M. T., Pelegrin, P. & Surprenant, A. (2006) Identification of Thr 283 as a key determinant of P2X 7 receptor function. Br J Pharmacol 149 (3):261-268. 10.1038/sj.bjp.0706880

43 Donnelly-Roberts, D. L., Namovic, M. T., Han, P. & Jarvis, M. F. (2009) Mammalian P2X7 receptor pharmacology: comparison of recombinant mouse, rat and human P2X7 receptors. Br J Pharmacol 157 (7):1203-1214. 10.1111/j.1476-5381.2009.00233.x

44 Simpson, E. M., Linder, C. C., Sargent, E. E., Davisson, M. T., Mobraaten, L. E. & Sharp, J. J. (1997) Genetic variation among 129 substrains and its importance for targeted mutagenesis in mice. Nat Genet 16 (1):19-27. 10.1038/ng0597-19

45 Beck, J. A., Lloyd, S., Hafezparast, M., Lennon-Pierce, M., Eppig, J. T., Festing, M. F. W. & Fisher, E. M. C. (2000) Genealogies of mouse inbred strains. Nat Genet 24 (1):23-25. 10.1038/71641

46 Johnson-Huang, L. M., Suárez-Fariñas, M., Pierson, K. C. *et al.* (2012) A single intradermal injection of IFN-γ induces an inflammatory state in both non-lesional

psoriatic and healthy skin. J Invest Dermatol 132 (4):1177-1187. 10.1038/jid.2011.458

47 Burrell, H. E., Wlodarski, B., Foster, B. J., Buckley, K. A., Sharpe, G. R., Quayle, J. M., Simpson, A. W. M. & Gallagher, J. A. (2005) Human Keratinocytes Release ATP and Utilize Three Mechanisms for Nucleotide Interconversion at the Cell Surface. J Biol Chem 280 (33):29667-29676. 10.1074/jbc.M505381200

48 Burnstock, G., Knight, G. E. & Greig, A. V. H. (2012) Purinergic signaling in healthy and diseased skin. J Invest Dermatol 132 (3.1):526-546. 10.1038/jid.2011.344

FIGURE LEGENDS

Figure 1 IMQ treatment induces greater ear swelling in BALB/c mice compared to C57BL/6 mice.

(**a-b**) Aldara™ cream (containing 5% IMQ) was applied to one ear of BALB/c and C57BL/6 mice from day 0 to 5. Contralateral ears were left untreated (control). (**a**) Ear swelling was measured over 6 days. Data represents group means ± SEM (n = 14 per strain). *** P < 0.0001 compared to C57BL/6. (**b**) Ears from mice at end-point were stained with haematoxylin and eosin, and viewed by microscopy. Each image is representative of 14 mice per group. Bars represent 200 μm. (**c**) Epidermal thickness was measured on histological images using ImageJ. Data represents group means ± SEM (n = 14 mice per group); symbols represent individual ears; *** P < 0.0001 compared to corresponding control.

Figure 2 P2X7 is up-regulated in IMQ-treated skin and IMQ can induce ATP release from keratinocytes.

(**a**) P2X7 expression in untreated (control) and IMQ-treated ears from BALB/c and C57BL/6 mice at end-point (Fig. 1) was assessed by qPCR. Data represents group means ± SEM (n = 5 mice per strain); symbols represent individual ears; * P < 0.05, *** P < 0.0001 compared to corresponding control. (**b and c**) Human HaCaT keratinocytes were incubated in DMSO or 1 μg/mL IMQ for 30 min and (**b**) ATP release assessed using a bioluminescence assay, and (**c**) LDH release was assessed using a spectrophotometric assay. Data represents group means ± SEM (n = 9 from three individual experiments); * P < 0.05 compared to DMSO.

Figure 3 BBG does not prevent IMQ-induced psoriasis-like inflammation.

(**a**) Murine J774 macrophages were incubated for 15 min at 37°C in the absence or presence of 10 μM BBG, and then with 25 μM ethidium bromide in the absence or presence of 1 mM ATP for 10 min at 37°C. Assays were stopped by addition of $MgCl_2$ medium, and ethidium$^+$ uptake was then assessed by flow cytometry. Data represents group means ± SEM (n = 3); * P < 0.05, *** P < 0.0001 compared to corresponding basal. (**b-d**) Aldara^{TM} cream (containing 5% IMQ) was applied to one ear of BALB/c mice from day 0 to 5. Contralateral ears were left untreated (control). Mice were injected i.p. with BBG or saline (control) on days 0, 2, and 4. (**b**) Ear swelling was measured over 6 days. Data represents group means ± SEM (n = 5 mice per treatment); ** P < 0.005 compared to BBG. (**c**) Ears from mice at end-point were stained with haematoxylin and eosin, and viewed by microscopy. Each image is representative of 5 mice per treatment. Bars represent 200 μm. (**d**) Epidermal thickness was measured on histological images using ImageJ. Data represents group means ± SEM (n = 5 mice per treatment); symbols represent individual ears; *** P < 0.0001 compared to corresponding control.

Figure 4 A-804598 does not prevent IMQ-induced psoriasis-like inflammation.

(**a**) Murine J774 macrophages were incubated for 15 min at 37°C in the absence or presence of 1 μM A-804598, and then with 25 μM ethidium bromide in the absence or presence of 1 mM ATP for 10 min at 37°C. Assays were stopped by addition of $MgCl_2$ medium, and ethidium$^+$ uptake was then assessed by flow cytometry. Data represents group means ± SEM (n = 3); *** P < 0.0001 compared to corresponding basal. (**b-d**) Aldara^{TM} cream (containing 5% IMQ) was applied to one ear of BALB/c mice from day 0 to 5. Contralateral ears were left untreated (control). Mice were injected i.p. with A-804598 or DMSO (control) on days 0 and 2. (**b**) Ear swelling was measured over 6 days. Data represents group means ± SEM (n =

5 mice per treatment). (**c**) Ears from mice at end-point were stained with haematoxylin and eosin, and viewed by microscopy. Each image is representative of 5 mice per treatment. Bars represent 200 μm. (**d**) Epidermal thickness was measured on histological images using ImageJ. Data represents group means ± SEM (*n* = 5 mice per treatment); symbols represent individual ears; *** $P < 0.0001$ compared to corresponding control.

Figure 5 Genetic deletion of P2X7 does not prevent IMQ-induced psoriasis-like inflammation.

(**a-c**) Aldara^{TM} cream (containing 5% IMQ) was applied to ears of C57BL/6 and P2X7 KO mice from day 0 to 5. Contralateral ears were left untreated (control). (**a**) Ear swelling was measured over 6 days. Data represents group means ± SEM (*n* = 10 mice per strain). (**b**) Ears from mice at end-point were stained with haematoxylin and eosin, and viewed by microscopy. Each image is representative of 10 mice per group. Bars represent 200 μm. (**c**) Epidermal thickness was measured on histological images using ImageJ. Data represents group means ± SEM (*n* = 10 mice per strain); symbols represent individual ears; *** $P < 0.0001$ compared to corresponding control.

Figure 6 IMQ-induced leukocyte infiltration is similar in C57BL/6 and P2X7 KO mice.

(**a-d**) Single whole ear cell suspensions of ears from untreated (control) and IMQ-treated C57BL/6 and P2X7 KO mice at end-point (Fig. 5) were labelled with fluorochrome-conjugated mAb and analysed by four-colour flow cytometry. Data represents total numbers of group means ± SEM for (**a**) leukocytes ($CD45^+$), (**b**) neutrophils ($CD45^+$ $Ly6G^+$ $CD11b^+$) (**c**) macrophages ($CD45^+$ $Ly6G^-$ $CD11b^+$), and (**d**) T cells ($CD45^+$ $CD3^+$) in each cell suspension (*n* = 5 mice per group); symbols represent individual ears; ** $P < 0.005$, *** $P < 0.0001$ compared to respective control ears.

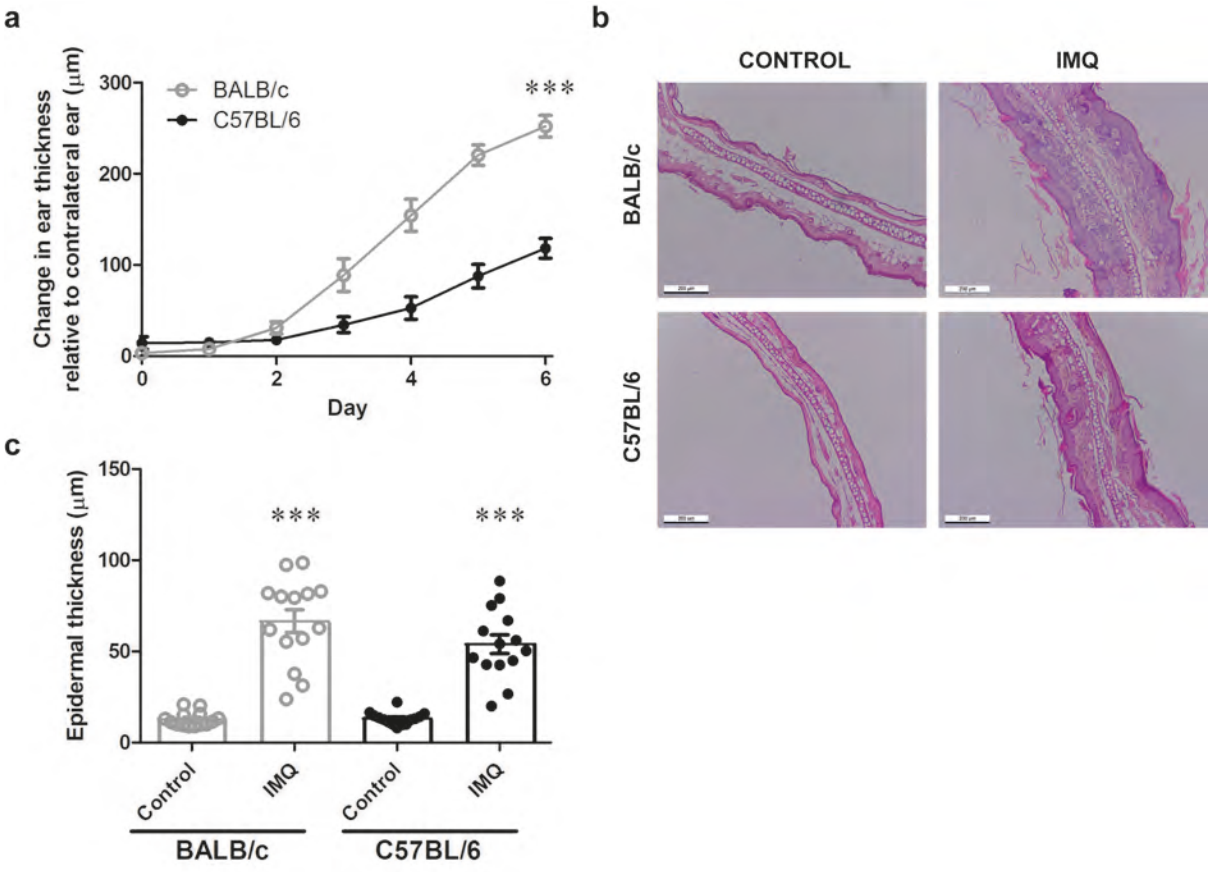
a
Change in ear thickness relative to contralateral ear (μm)
300
200
100
0
BALB/c
C57BL/6
***
0
2
4
6
Day
b
CONTROL
IMQ
BALB/c
C57BL/6
c
Epidermal thickness (μm)
150
100
50
0
***
***
Control
IMQ
Control
IMQ
BALB/c
C57BL/6

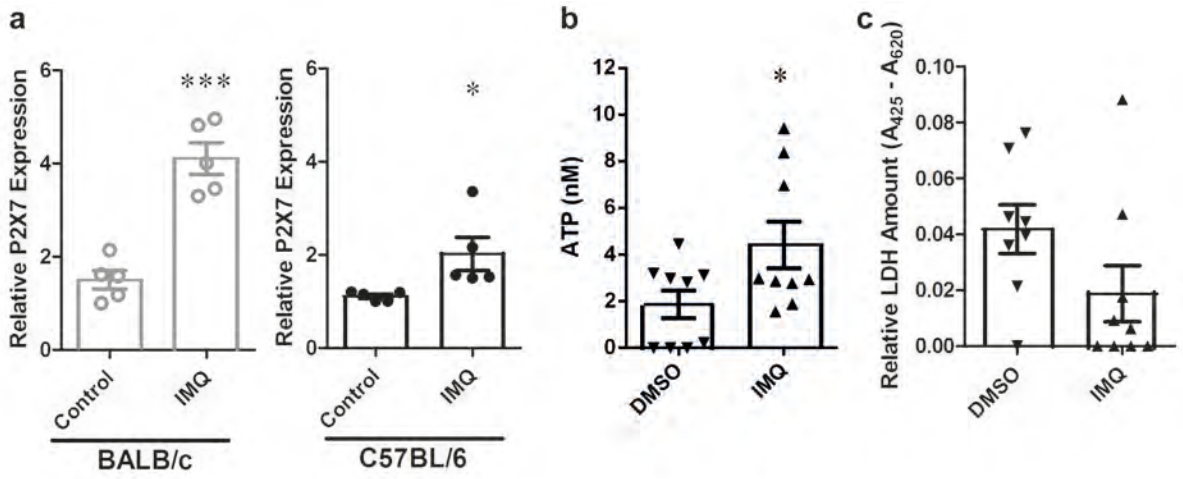
a
Relative P2X7 Expression
6
4
2
0
***
Control
IMQ
BALB/c
Relative P2X7 Expression
6
4
2
0
*
Control
IMQ
C57BL/6
b
ATP (nM)
12
10
8
6
4
2
0
*
DMSO
IMQ
c
Relative LDH Amount (A_{425} - A_{620})
0.10
0.08
0.06
0.04
0.02
0.00
DMSO
IMQ

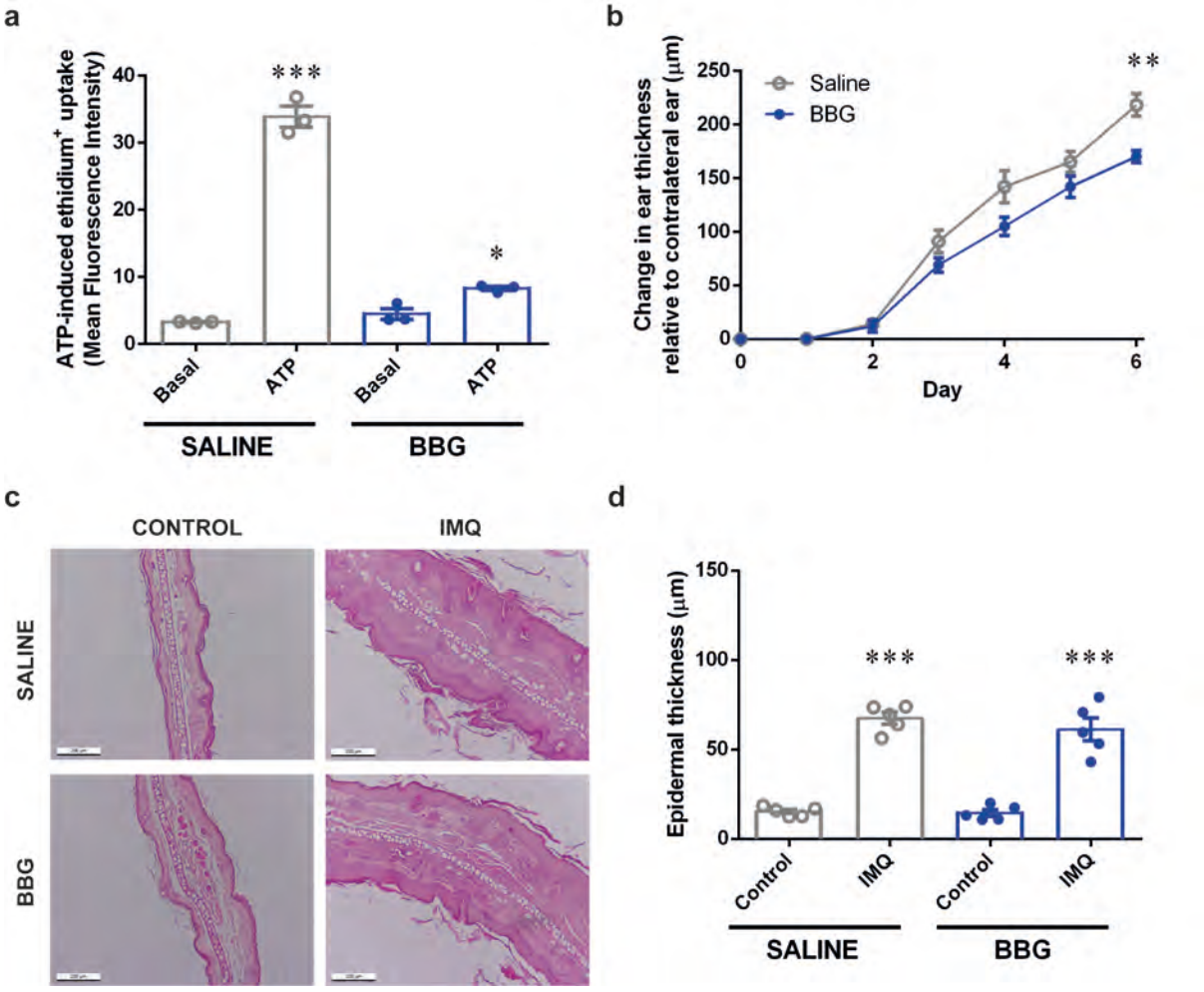
a
ATP-induced ethidium+ uptake (Mean Fluorescence Intensity)
40
30
20
10
0
***
*
Basal
ATP
Basal
ATP
SALINE
BBG
b
Change in ear thickness relative to contralateral ear (μm)
250
200
150
100
50
0
Saline
BBG
**
0
2
4
6
Day
c
CONTROL
IMQ
SALINE
BBG
d
Epidermal thickness (μm)
150
100
50
0
***
***
Control
IMQ
Control
IMQ
SALINE
BBG

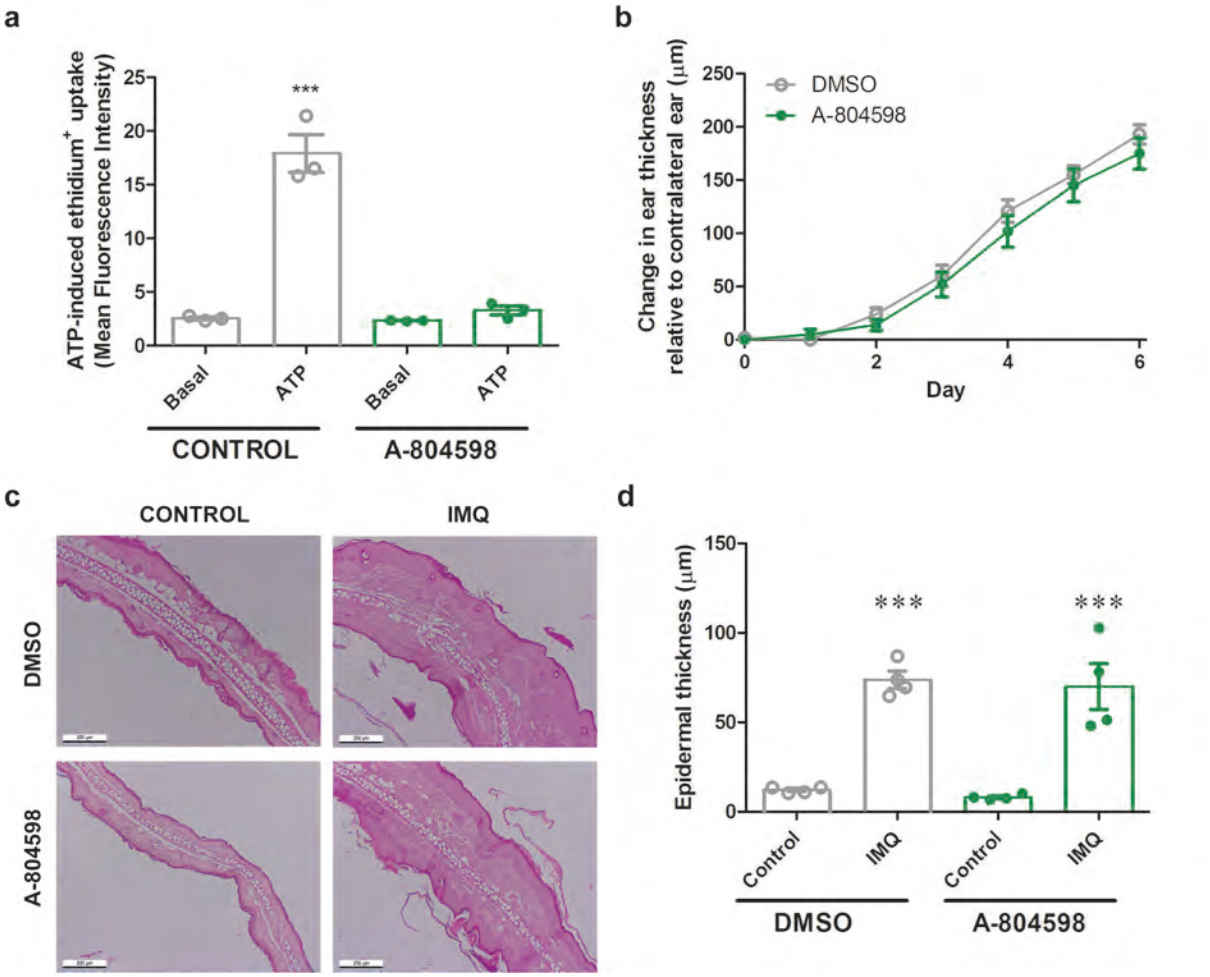
a
ATP-induced ethidium+ uptake (Mean Fluorescence Intensity)
25
20
15
10
5
0
***
Basal
ATP
Basal
ATP
CONTROL
A-804598
b
Change in ear thickness relative to contralateral ear (μm)
250
200
150
100
50
0
DMSO
A-804598
0
2
4
6
Day
c
CONTROL
IMQ
DMSO
A-804598
d
Epidermal thickness (μm)
150
100
50
0
***
***
Control
IMQ
Control
IMQ
DMSO
A-804598

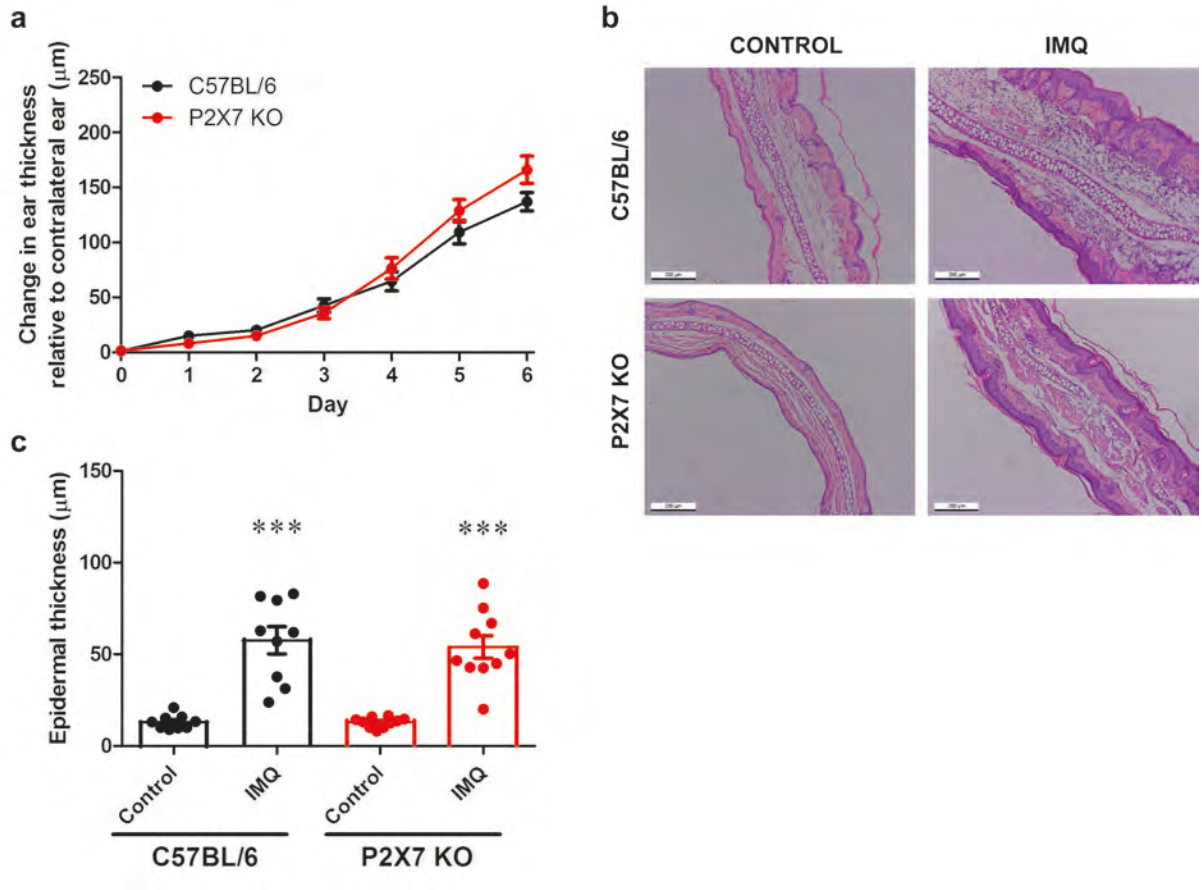
a
Change in ear thickness relative to contralateral ear (μm)
C57BL/6
P2X7 KO
Day
b
CONTROL
IMQ
C57BL/6
P2X7 KO
c
Epidermal thickness (μm)
***
***
Control
IMQ
Control
IMQ
C57BL/6
P2X7 KO

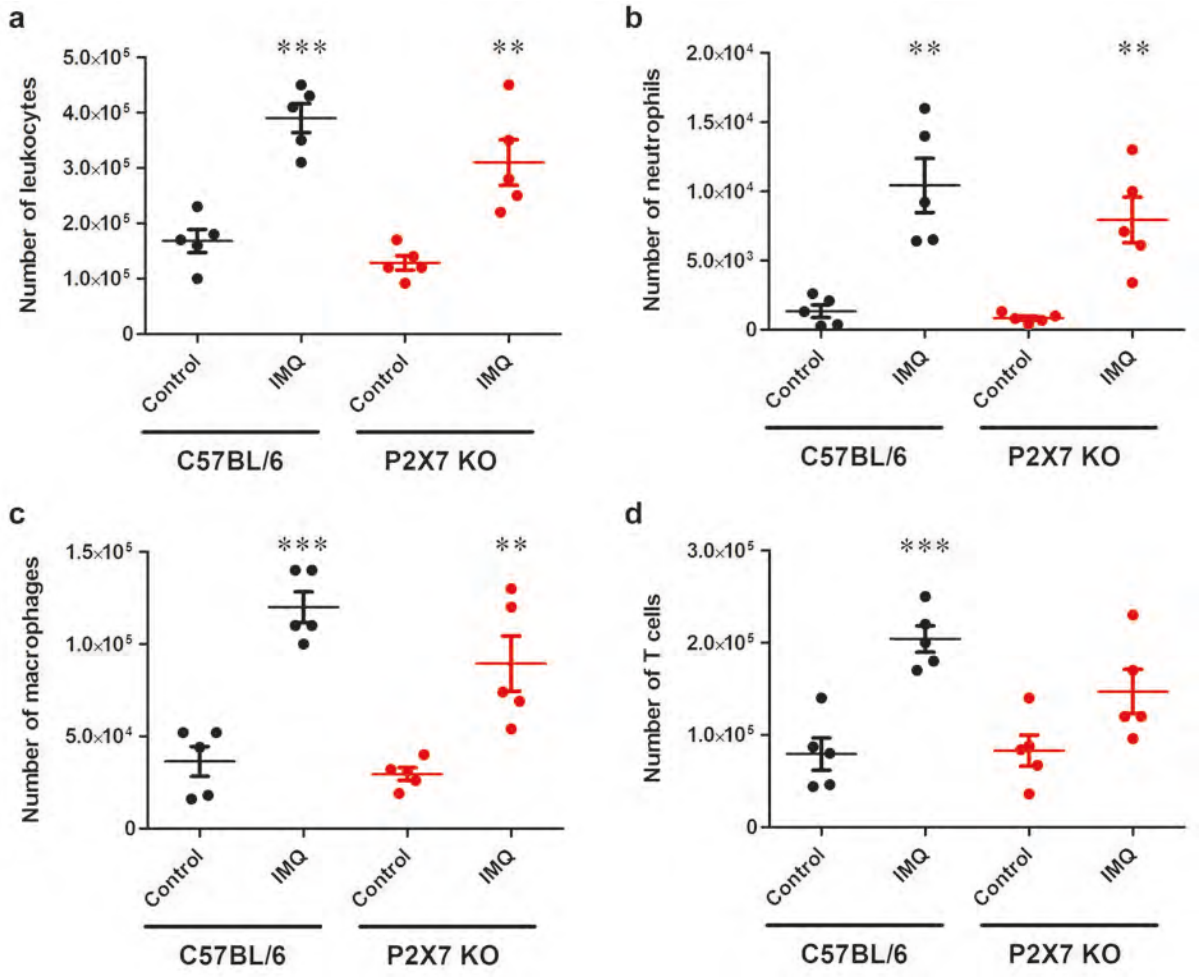
a
Number of leukocytes
5.0×10⁵
4.0×10⁵
3.0×10⁵
2.0×10⁵
1.0×10⁵
0
***
**
Control
IMQ
Control
IMQ
C57BL/6
P2X7 KO
b
Number of neutrophils
2.0×10⁴
1.5×10⁴
1.0×10⁴
5.0×10³
0
**
**
Control
IMQ
Control
IMQ
C57BL/6
P2X7 KO
c
Number of macrophages
1.5×10⁵
1.0×10⁵
5.0×10⁴
0
***
**
Control
IMQ
Control
IMQ
C57BL/6
P2X7 KO
d
Number of T cells
3.0×10⁵
2.0×10⁵
1.0×10⁵
0
***
Control
IMQ
Control
IMQ
C57BL/6
P2X7 KO